Ore Geology Reviews 120 (2020) 103466

Contents lists available at ScienceDirect

Ore Geology Reviews

journal homepage: www.elsevier.com/locate/oregeorev

Primary study of germanium isotope composition in sphalerite from the Fule Pb–Zn deposit, Yunnan province

Taotao Liu[a,b], Chuanwei Zhu[a,*], Guangshu Yang[c,d,*], Guishan Zhang[b], Haifeng Fan[a], Yuxu Zhang[a], Hanjie Wen[a]

[a] State Key Laboratory of Ore Deposit Geochemistry, Institute of Geochemistry, Chinese Academy of Sciences, Guiyang 550081, Guizhou, China
[b] College of Earth Science and Resources, Chang'an University, Xi'an 710054, Shannxi, China
[c] Kunming University of Science and Technology, Kunming 650093, China
[d] Faculty of Land Resources Engineering, Kunming University of Science and Technology, Kunming 650093, Yunnan, China

ARTICLE INFO

Keywords:
Dispersed elements
Ge isotope
Sphalerite
Fule Pb–Zn deposit

ABSTRACT

The Sichuan–Yunnan–Guizhou metallogenic province in southwest China is one of the most important low-temperature metallogenic domains in the country, and more than 400 Pb–Zn deposits and/or mineralization points are located in this area. The Fule deposit is better known that the other Pb–Zn deposits in the region because it is extremely highly enriched with dispersed elements, including Ge, Ga, and Cd. Based on information obtained from our previous studies, the contents of Ge and its isotopic compositions in sphalerite are investigated herein. Results show that the Ge content ranges from 60 ppm to 141.5 ppm, and $\delta^{74/70}$Ge values vary from −6.57‰ to 0.97‰. In this respect, −6.57‰ is the most negative Ge isotope composition value reported in any sphalerite or seafloor sulfides to date. The Cd and Ge contents in sphalerite have a good negative relationship, and it is suggested that the mechanisms of Cd and Zn substitution are responsible for the low incorporation of Ge and relate to the high Cd content (up to 3%) of the sphalerite. In addition, there is a good positive correlation between the Ge contents and δ^{34}S values, which was likely triggered by variations of fluid temperature. In the same hand specimen, light Ge isotope is more likely to be enriched in dark sphalerite rather than light sphalerite, similarly to Cd isotope distribution in dark and light-colored sphalerite. In addition, Cd and Ge isotope compositions, measured in an ore profile from SBFL22 to SBFL26, show a good positive relationship, suggesting that the fractionation mechanisms between Cd and Ge isotopes may be similar and they were controlled by kinetic fractionation during sphalerite precipitation. Based upon previous limited studies, we conclude that Ge in the Fule deposit is derived from mixing sources and sediment is likely the dominant one.

1. Introduction

Germanium (Ge) is a typical dispersed element that has minor content variations within different end-members on Earth, such as 1.1–1.3, 1.4–1.5, and 1.4–1.6 ppm within the primitive mantle, oceanic crust, and continental crust, respectively (Taylor and McClennan, 1985; Tu et al., 2003). It exhibits lithophile, chalcophile, siderophile, and organophile behaviors in these various geological environments (Höll et al., 2007; Zhu et al., 2014), which can be confirmed that industrial Ge is mainly sourced from coal and Pb–Zn deposits, such as the Lincang Ge-rich coal deposit and the giant Huize Pb–Zn–Ge deposit.

The Sichuan–Yunnan–Guizhou (SYG) area is one of the largest Pb-Zn producers in China, and more than 10 large-scale (e.g., the Huize) and up to 400 medium- and small-scale Pb–Zn deposits were discovered in the past decades (Huang et al., 2004; Hu et al., 2017; Cui et al., 2018). Geologically, the deposits are located in the southwest margin of the Yangtze block, and most of them are distributed within a triangular region limited by the Anning River fault, the Shizong–Mile fault, and the Yadu–Ziyun fault (Fig. 1). Interestedly, most deposits in this area are rich in dispersed elements, including Ge, Cd, Se, and Ga, this metallogenic province is also well known (both within China and globally) for its dispersed element resources (Tu et al., 2003). Researches have focused on Ge sources in this area for decades (e.g., Tu et al., 2003; Zhang et al., 2012; Meng et al., 2015), most studies were investigated the Ge concentrations and occurrences and found that sphalerite is the only Ge-bearing sulfide with concentrations up to ~ 200 ppm (Si, 2005; Zhang et al., 2012; Zhu, 2014; Zhu et al., 2017). However, the sources and the enrichment mechanisms of Ge in the deposits are still not well

* Corresponding authors.
E-mail addresses: zhuchuanwei@mail.gyig.ac.cn (C. Zhu), 13888600582@163.com (G. Yang).

https://doi.org/10.1016/j.oregeorev.2020.103466
Received 20 May 2019; Received in revised form 9 December 2019; Accepted 12 March 2020
Available online 14 March 2020
0169-1368/

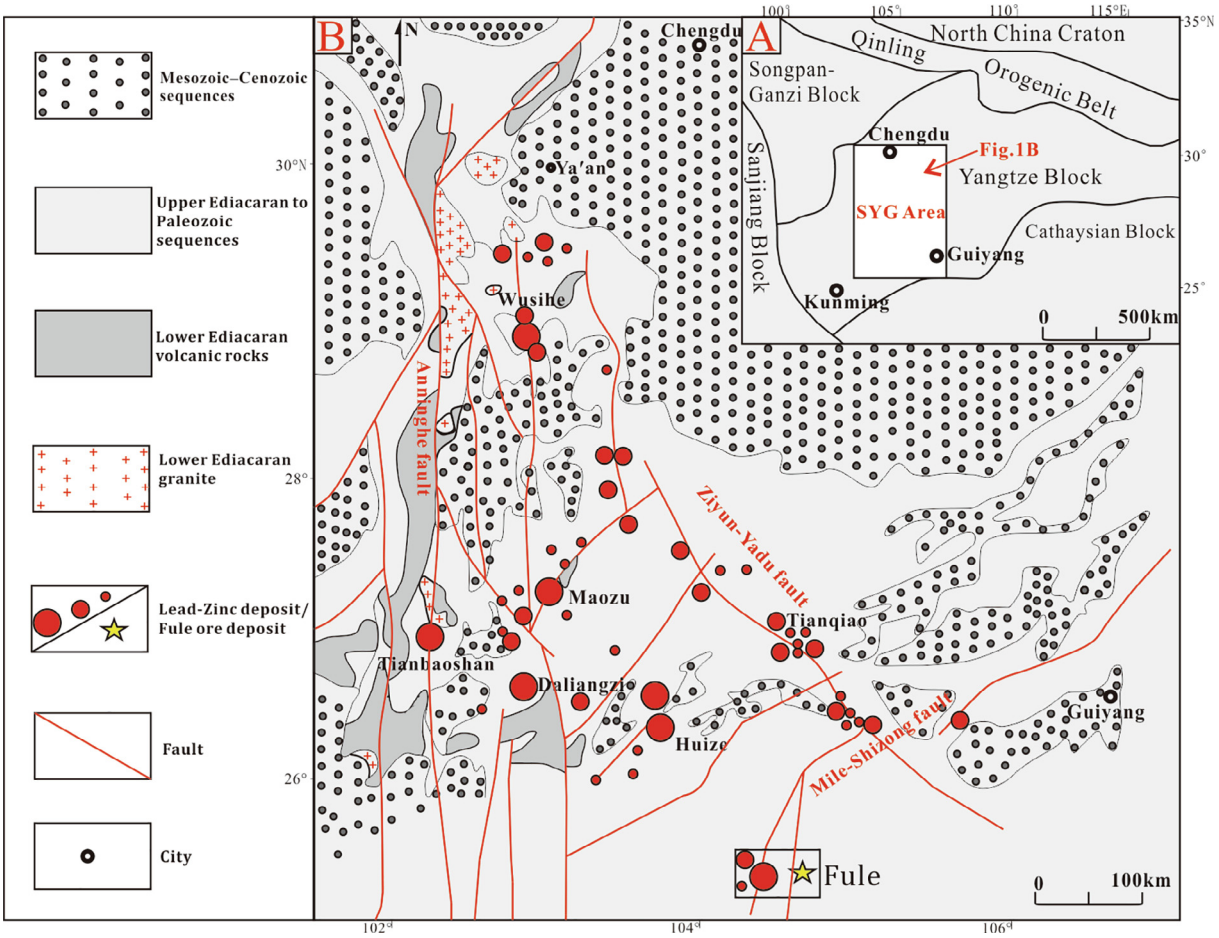

Fig. 1. (A) Tectonic sketch and (B) regional geological map of the Sichuan–Yunnan–Guizhou Pb–Zn metallogenic province, SW China (modified from Xiong et al., 2018).

understood.

Due to its largest Zn source in the SYG area, the Huize deposit has the largest Ge sources, however, the highest Ge concentrations in sphalerite were occurred in the Fule deposit basing on the reported data (up to 200 ppm) (Zhang et al., 2012; Zhu, 2014; Meng et al., 2015). Interestedly, sphalerite from the Fule deposit also has the highest Cd, Se and Ga concentrations, with respective values of up to 34981 ppm, 177 ppm, and 358 ppm (Si, 2005; Zhang et al., 2012; Zhu, 2014; Zhu et al., 2017). Previous studies have focused on the mineralogical characteristics of the deposit (Si, 2005; Liang et al., 2016; Li et al., 2018), the enrichment rules and mechanisms of dispersed elements (Si et al., 2006; Zhang et al., 2012), the ore-forming ages (Liu et al., 2015; Cui et al., 2018), the relationships between structure and mineralization (Lü et al., 2015), and the features of the ore-forming fluids (Nian et al., 2017; Zhou et al., 2018). These studies make the Fule deposit as an ideal deposit to study the potential applications of Ge isotope in a hydrothermal system in the SYG area.

Germanium has five stable isotopes in nature, ^{70}Ge, ^{72}Ge, ^{73}Ge, ^{74}Ge, and ^{76}Ge, with relative abundances of 21.2%, 27.7%, 7.7%, 35.9%, and 7.5%, respectively (Green et al., 1986; Rosman and Taylor, 1998; Rouxel and Luais, 2017). Pilot studies of the Ge isotopic system date back to the 1950s (Reynolds, 1953), but the analytical precision obtained was extremely limited for years. However, in the past few decades, with the advent of high precision mass spectrometry (e.g., MC-ICP-MS and TIMS) and the update of analytical methods, the Ge isotope analytical precision has been significantly improved. It is thus possible to measure minor changes in the Ge isotope induced by different geological processes involving its transportation and deposition in nature (e.g., Rouxel et al., 2006; Siebert et al., 2006; Qi et al., 2011, 2019; Escoube et al., 2012, 2015; Belissont et al., 2014; Meng et al., 2015; Luais 2012; Baronas et al., 2017, 2018; Meng and Hu, 2017), and the Ge isotope could therefore be a powerful tool used to track sources of Ge in hydrothermal systems (Rouxel and Luais, 2017).

Combined with the results of our previous study (Zhu et al., 2017), the Ge isotope was used in this study as a major tool to constrain Ge isotope fractionation mechanisms and sources of Ge in the Fule deposit. The results provided here will give a better understanding of Ge enrichment in this deposit and other deposits located in the SYG area.

2. Geological setting

2.1. Regional geology

The Sichuan–Yunnan–Guizhou metallogenic province is situated in the southwestern margin of the Yangtze block. It is located at the transition zone between Gondwanaland and Laurasia (Liu et al., 2004) and is adjacent to the Songpan-Ganzi block in the north, the South China fold belt in the south, and the Sanjiang fold belt in the west (Fig. 1A). The Yangtze block has been part of long-term geological evolutionary processes over time and of the many tectonic disintegrations and mosaic formations of Pangea that has been accompanied by multi-stage tectonism, magmatism, metamorphism, and deformation (Liu et al., 2004). The strata outcropped in the low-temperature ore-forming domain of Sichuan–Yunnan–Guizhou province are complete and have a distinct binary model, and occur as structural layers of crystalline basements and sedimentary covers (Jing, 2008). The structural layer of basements consists mainly of high-grade metamorphic basement complexes, with Proterozoic metamorphic volcanics above

the metamorphic complexes. There is a tectonic layer of fold basements under the Sinian strata that includes the Kangding Group, Huili Group, and Kunyang Group. They are divided into three stratums from bottom to top: the lower bed is principally Archean Eonothem-Palaeoproterozoic moderate and high-grade metamorphic complexes; the middle layer is mainly Mesoproterozoic metamorphosed fine clastic rocks interbedded with metamorphic volcanic sedimentary rocks; and the upper stratum is predominantly Neoproterozoic carbonate rocks and low-grade metamorphic clastic rocks. The formations of these fold basements are mainly exposed in districts such as Dongchuan in the Yunnan Province and Huidong and Huili in the Sichuan Province. The cover sequences from Sinian to Quaternary systems are well developed, and the sedimentary rock lithologies are dominated by carbonate rocks, followed by shale and sandstone. Of these sequences, the Carboniferous, Permian, and Triassic formations are characterized by their continuous exposure, wide distribution, and large sedimentary thicknesses. The largest igneous event in the region is evidenced in the Emeishan flood basalts of the middle-late Permian, and many deposits located in this district are overlain by the basalts (Zhou et al., 2013). Although small-scale magmatism occurs more frequently, and is mainly intruded diabase, it occurs on a smaller scale than the Emeishan basalts in the middle-late Permian. There are also evident stages of tectonic activity in the area, which has formed anticlines, synclines, domes on different scales, and NE-, NS- and NW-striking faults that play a key role in controlling the distribution of the Pb–Zn deposit. (Fig. 1B; Huang et al., 2004).

2.2. Deposit geology

The Fule Pb–Zn deposit is hosted in the Maokou Formation(P_1 m) and the strata exposed in the ore field are mainly composed of (from old to new) (Fig. 2A): (1) the Carboniferous Maping Formation (a set comprising dolomitic bioclastic limestone, fine grained limestone, and a small amount of dolomite mingled with quartz sandstone); (2) Permian strata including the Liangshan (limestone, shale, and quartz fine sandstone) and Maokou Formations (limestone inter-layered with dolomite), Emeishan flood basalts, and the Xuanwei Formation (an important coal-bearing formation in this district); (3) the Triassic Feixianguan (sandstone, argillaceous limestone, siltstone, and shale) and Jialingjiang Formations (clastic rock and medium-thick layered limestone); (4) the lithology of Quaternary strata that mainly consists of sandy clay and is scattered throughout the valley.

The mining district covers an area of approximately 4.5 km^2 (Si, 2005; Fig. 2A). There are more than 20 ore bodies in the Fule Pb–Zn deposit, which are hidden at a depth of approximately 150–200 m beneath the surface and are commonly distributed in a NW-SE direction. Most of the ore bodies are single-layer, but some have a two-layered texture, and they are lenticular, stratiform-like, and veined in shape, and appear slowly along layers or inter-laminar fissures (Fig. 2B). The occurrence of ore bodies is basically consistent with that of the strata, which are inclined in a SE direction at a dip of ~10°. However, there is no definite regularity to the pinch and swell of ore bodies. Ore body thicknesses vary greatly, sulfide enrichment is heterogeneous, and the bodies occur on diverse scales. Large bodies are mainly distributed in the center of deposits, and smaller bodies lie on the outer side of the large ore bodies in the form of a lens-shaped “satellite”. However, regardless of scale, the plane features of the ore bodies are irregular.

The ore types are mainly primary, and large amounts of oxidized ore is only seen in the late periods at fracture sites. Mineral assemblages are simple, and sphalerite and galena are the dominant minerals mined on an industrial scale, which account for more than 99% of the total amount of metal minerals, whereas pyrite, chalcopyrite, tetrahedrite, and zinc-tennantite (newly discovered by Li et al., 2018) are relatively minor. More than 99% of gangue minerals are comprised of dolomite and calcite. The oxidized ores are mainly composed of two kinds of smithsonite: a large amount of smithsonite with a framework texture formed by the oxidation of sphalerite; and a small amount of layered smithsonite precipitated from oxidized fluids (Zhu et al., 2017; Zhu et al., 2018). In addition, small amounts of secondary minerals, such as hydrozincite, azurite, malachite, and anglesite, are found in the oxidized ore. However, the total amount of secondary minerals from oxided ore generally comprises less than 1% of its total (Zhu et al., 2018). The primary ore minerals commonly have coarse-grained textures and euhedral–subhedral textures, but they have also developed giant crystal euhedral, medium-grained, and fine-grained textures; and all these textures appear in sphalerite, galena, dolomite and calcite. A co-edge texture is also developed, and it occurs mostly in mineral pairs such as sphalerite and galena, dolomite and galena, sphalerite and dolomite. The primary ore minerals predominantly have brecciated, massive, spotted, disseminated, and veined structures. The main minerals and their occurrence are presented in detail as following:

Sphalerite usually appears in calcite and dolomite in the form of a lump, mass, or spot, and has a disseminated distribution. Most sphalerite has a subhedral coarse-grained texture, the grains of which are generally 2–3 mm. However, a few sphalerites have fine granular (less than 1 mm) and medium granular textures (1–2 mm), and macrocrystalline sphalerite (greater than5 mm) can be seen locally. The color is an important mineral typomorphic characteristic of sphalerite, which is mainly light-brown and dark-brown sphalerite, but light-yellow sphalerite is minor. The color gradation was suggested to determine the formation sequence of the sphalerite. Generally, dark sphalerite was formed earlier than light sphalerite, such as sphalerite from the Huize Pb–Zn deposit (Han et al., 2007; Zhou et al., 2014). In the Fule deposit, the dark-brown sphalerite is cross-cut by light sphalerite at a microscopic scale, which confirms the late formation of light sphalerite (Zhu et al., 2017). The sphalerite color has a certain regularity within the Fule Pb–Zn deposit: throughout the entire deposit, the color of deep partial sphalerite is darker than that of shallow positional sphalerite; and for a single ore body, the color of the middle part of the ore body is relatively darker than that of the periphery (Si, 2005). Along the direction of ore body thickness, the lower part is darker than the upper part; for ores of different grade, rich ore is darker than poor ore; for individual ores, the color of sphalerite is lighter in relation to its proximity to gangue (Si, 2005; Zhu, 2014).

Galena is the second-most important metallic mineral in the deposit. Galena common occurs with massive and lumpy structures, but a few have a disseminated structure. In addition, spotted and banded structures can also be seen in galena that hosted in sphalerite. Similar to sphalerite, galena also has a euhedral texture (a cubic form), but distorted and subhedral-xenomorphic texture is minor. The grain size of galena varies greatly: most are between 2 mm and 10 mm, but a few with macro-crystalline textures have grain sizes larger than 100 mm, whereas those with disseminated textures are approximately only 1 mm.

Dolomite has a massive structure and a few occurring in sphalerite are lumpy, banded, and veined. Relatively less dolomite is distributed in the middle of the ore body than at the edge, and there is relatively more in the upper part than in the lower (Fig. 3). Dolomite is closely associated with sphalerite and galena.

Calcite in the ore body mainly has a lumpy structure with minor as veined structure. In addition, a small amount appears in dolomite and sphalerite with a banded structure. Calcite is pure and has a macrocrystalline texture with a grain size of 5–30 mm. Calcite produced in veins commonly has a subhedral texture with grain size less than 1 mm. Veined calcite usually cuts across the lumpy sphalerite and galena. Macro-crystalline white calcite is distributed within the massive pure white dolomite.

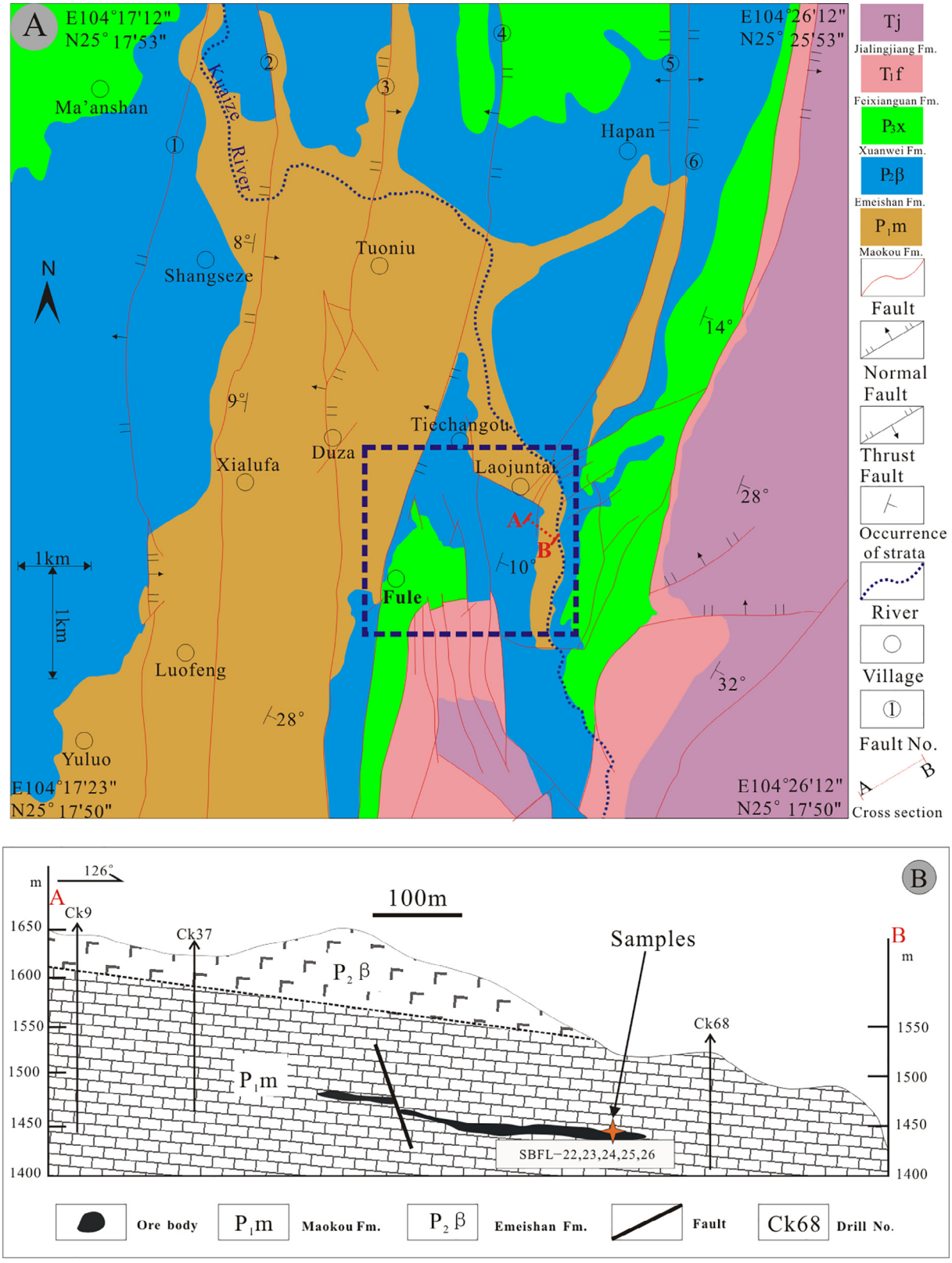

Fig. 2. (A) Regional geological map and (B) sketched cross-section of Fule Pb–Zn deposit (modified from Zhu et al., 2017).

3. Samples and methods

3.1. Sample collection and preparation

In this study, five Pb–Zn (SBFL22 to SBFL26) ore samples were collected at a sulfide profile from the No. 78 (height, 1445 m) ore body, and two samples (SBFL17, SBFL18) were collected from other two different ore bodies. The metal reservoir of the No. 78 ore body is the largest one within the Fule Pb–Zn deposit. There are regular changes in the mineral assemblage from the bottom to the top of the ore body, and

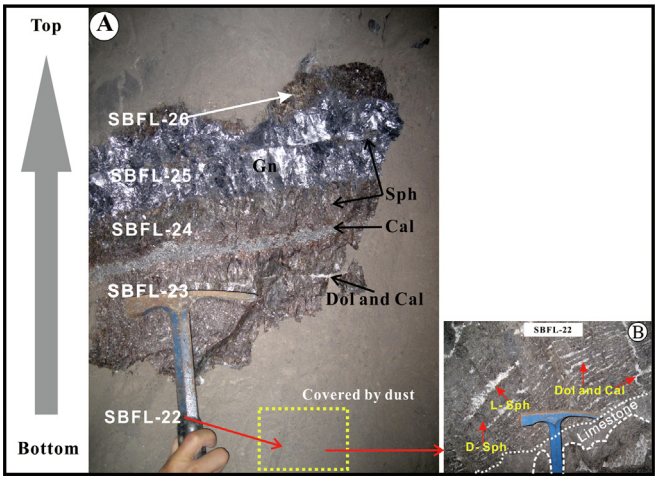

Fig. 3. Photograph of profile of No. 78 ore body and the positions where the five samples were collected in this research. (A) Panorama of No. 78 ore body; (B) close-up image of SBFL-22 from No. 78 ore body. Abbreviations are as follows: Sph: sphalerite, Cal: calcite, Gn: galena, Dol: dolomite, SBFL-22: Sample No, D-Sph: dark sphalerite, L-Sph: light sphalerite. Yellow rectangle represents location of amplified image within No. 78 ore body. (For interpretation of the references to color in this figure legend, the reader is referred to the web version of this article.)

in the color of sphalerite within ores. It is thus that the profile can be divided into five layers from lower to upper. In general, the bottom of the ore body is rich in dark sphalerite, while the upper part is rich in light sphalerite. A detailed description of the mineral assemblages and textures of studied samples are shown in Table 1 and Fig. 3. The SBFL-17 and SBFL-18 samples were obtained from another two ore bodies and were collected in the middle part of the 1406 level.

Samples were crushed to a 40–60 mesh, and washed with deionized water. Different colors of pure sphalerite were then handpicked under a binocular microscope. As reported previously (Zhang et al., 2012), sphalerite is the dominant Ge-bearing sulfide in this deposit, and other sulfide (e.g., galena) commonly contains sphalerite micro-inclusions as suggested by Zhu et al. (2017); it is impossible to obtain pure enough sulfide (e.g., galena) without sphalerite micro-inclusions, thus, we only measured Ge isotope compositions in sphalerite.

3.2. Ge isotope analyses

Prior to Ge isotope analyses, all pure mineral samples were crushed to less than a 200-mesh using an agate mortar. Samples weighing approximately 100 mg sphalerite were placed into a Teflon digestion vessel and then reacted with 3 mL of concentrated HNO_3 at 85 °C for ~24 h. After heating to dryness, samples were dissolved in 5 mL 1% HNO_3 (v/v) and then centrifuged at 4000 r/min for 10 min. 2 mL of the supernatant were transferred for Ge content measurements, and another 2 mL of supernatant were transferred for Ge purification. The two-step separation method for both the anion- and cation-exchange resins was employed for Ge purification as described in Zhu et al. (2014) (Table 2), and potential isobaric interferences were negligible in comparison with Ge concentrations, for example, the progressed samples have large Ge/Zn ratios (> 40) with Ge recovery of ~100% (Zhu et al., 2014).

Table 2
Sample digestion and column chemistry protocol.

Purification protocol	Volume (mL)	Remarks
AG1-X8 (100–200 mesh)	1.8	
1.4 mol/L HNO_3	10	Elution
Milli-Qwater	4	Elution
1 mol/L HF	10	Elution
Sample	2	
1 mol/L HF	5	Elution
Milli-Qwater	2	Elution
1.4 mol/L HNO_3	10	Collection
AG50W-X8 (200–400 mesh)	2	
0.14 mol/L HNO_3	10	Elution
Sample	2	Collection
0.14 mol/L HNO_3	4	Collection

Chemical separation and purification of samples was conducted in an ultra-clean lab at the State Key Laboratory of Ore Deposit Geochemistry, Institute of Geochemistry, Chinese Academy of Sciences. Germanium concentrations were analyzed at the ALS minerals-ALS Chemex (Guangzhou) Co., Ltd., using a method with the code PS-02 and results were within a 10% error. The Ge isotope composition was measured using a Thermo-Scientific Neptune MC-ICP-MS at the State key Laboratory for Mineral Deposits Research of Nanjing University, and the JMC Ge reference standard solution was adopted (1000 + 3 mg/L; Johnson Matthey Company, JMC). Isotopic data are reported using the δ value per mille (‰) notation, which is defined as follows,

$$\delta^{*/70}\mathrm{Ge}\ (‰) = [(^{*}\mathrm{Ge}/^{70}\mathrm{Ge})_{\mathrm{sample}}/(^{*}\mathrm{Ge}/^{70}\mathrm{Ge})_{\mathrm{std}}) - 1] \times 1000 \quad (1)$$

where * denotes 74, 73, and 72 but not 76, that is because certain molecular interferences with $^{76}Ge^{+}$ (such as $^{38}Ar^{38}Ar$ + and $^{36}Ar^{40}Ar$ +) are not minimized by the MC-ICP-MS (Escoube et al., 2012; Galy et al., 2003; Rouxeland Luais, 2017) and the minimum abundance(^{76}Ge, 7.5%) relative to other nuclides such as ^{74}Ge (35.9%). Commonly, $\delta^{74/70}$Ge is generally used to represent the Ge isotopic composition, due to their larger natural abundances and relatively minor isobaric interference of masses (Meng et al., 2017). In addition, "std" refers to the reference standard used for testing.

At present, NIST3120a is suggested as the zero-value standard of Ge isotope, and the conversion of the value between JMC and NIST3120a is conducted using the following simplified equation (a detailed description is presented in Rouxel and Luais, 2017; Escoube et al., 2012),

$$\delta^{74/70}\mathrm{Ge}_{\mathrm{NIST3120a}} = \delta^{74/70}\mathrm{Ge}_{\mathrm{JMC}} - 0.32‰ \quad (2)$$

4. Results

The results of Ge content measurements and isotope compositions are listed in Table 3. To control data quality, a duplicate (SBFL-26) was analyzed in this study, and identical results were obtained within an uncertainty (Table 3), indicating the reliability of the processes used in

Table 1
Mineral features in No. 78 ore body (from bottom to top ore) in Fule Pb–Zn deposit.

Sample Number	Objects	Major structure of ore	Mineral assemblage
SBFL-26	Dark–Light Sp, minor amount of Gn	massive ore	Sp + Gn
SBFL-25	Gn, minor amount of Sp	massive ore	Gn + Sp
SBFL-24	Dark–Light Sp, minor amount of banded Gn hosted in Sp	massive ore	Sp + Gn
SBFL-23	Dark–Light Sp, minor amount of spotted Gn hosted in Sp	massive ore	Sp + Gn
SBFL-22	Dark–Light Sp, minor amount of Gn, veined Dol cross-cutting Sp	massive ore	Sp + Gn + Dol

Table 3
Cd and Ge contents associated with Ge, Cd, and S isotope compositions of sphalerite from Fule deposit.

Sample Number	Color	$\delta^{74/70}Ge_{JMC}$ ‰	2SD	$\delta^{73/70}Ge$ ‰	2SD	Ge ppm	$\delta^{74/70}Ge_{NIST3120a}$	$\delta^{114/110}Cd$* ‰	2SD*	Cd* ppm	$\delta^{34}S$* ‰
SBFL-17	Dark	−2.77	0.14	−2.14	0.07	130.9	−3.09				
SBFL-17	Light	−2.18	0.37	−1.69	0.11	139.8	−2.50				
SBFL-18	Dark	1.29	0.27	0.98	0.11	120.2	0.97				
SBFL-18	Light	0.83	0.26	0.57	0.06	60.9	0.51				
SBFL-22	Dark	−2.83	0.21	−2.30	0.09	131.7	−3.15	0.06	0.04	14,714	14.8
SBFL-22	Light	−0.91	0.10	−0.76	0.11	141.5	−1.23	0.52	0.04	9083	14.0
SBFL-23	Dark	−5.69	0.06	−4.57	0.04	124.6	−6.01	0.28	0.03	15,046	13.8
SBFL-23	Light	−2.61	0.35	−2.00	0.21	139.8	−2.93	0.43	0.04	13,735	14.0
SBFL-24	Dark	−3.54	0.18	−2.75	0.05	95.2	−3.86	0.33	0.01	18,479	12.8
SBFL-24	Light	−3.26	0.30	−2.55	0.07	85.5	−3.58	0.47	0.01	16,783	12.3
SBFL-25	Dark	−6.25	0.17	−4.77	0.10	96.1	−6.57	0.21	0.02	18,645	13.4
SBFL-26#	Dark	−3.63	0.04	−2.37	0.39	69.5	−3.95	0.46	0.08	34,981	11.7
SBFL-26#	Dark	−3.67	0.04	−2.88	0.13	70.4	−3.99	0.43	0.03	34,757	
JMC standard		0.04	0.23	0.02	0.16						

Where "#" = a pair of parallel samples and "*" represents data cited from Zhu et al. (2017).

treating samples and measuring Ge isotope ratios.

With respect to the position-relation diagram of tested samples and the theoretical mass fractionation curve (TMFL) of equilibrium and kinetic fractionation (Fig. 4), all samples (including the standard deviation) are seen to fall on the TMFL curve of equilibrium fractionation and kinetic fractionation, and it can be defined by the following equations (3) and (4), respectively (Young et al., 2002),

$$\delta^{73/70}Ge = (1/m_{73} - 1/m_{70}) / (1/m_{74} - 1/m_{70}) \times \delta^{74/70}Ge \approx 0.7607 \times \delta^{74/70}Ge, \quad (3)$$

$$\delta^{73/70}Ge = ln(m_{73} - m_{70}) / ln(m_{74} - m_{70}) \approx 0.7927 \times \delta^{74/70}Ge, \quad (4)$$

In addition, the slope of the fitted straight line is 0.7639 (correlation coefficient = 0.9929), which is between the slope of theoretical equilibrium fractionation (0.7607) and kinetic fractionation (0.7927), suggesting that the measured Ge isotope data are reliable.

Sphalerite from the Fule deposit has minor variations of Ge concentrations, which range from 60 ppm to 141.5 ppm; on the contrary, there are large Ge isotope fractionation with the $\delta^{74/70}$Ge values ranging from − 6.57‰ to 0.97‰, and the most negative values are lower than those of previously reported data in Pb–Zn deposits from SYG area (−4.94‰ to 2.07‰; Meng et al., 2015), the Noailha-Saint-Salvy Zn–Ge–Ag–(Pb–Cd) deposit (−2.07 to 0.91; Belissont et al., 2014) and the seafloor sulfides (−4.00‰ to − 2.98‰; Escoube et al., 2012). Interestedly, one sample (SBFL-25) from the Fule deposit has the lightest isotope compositions of Ge in sulfides in comparison with the reported data.

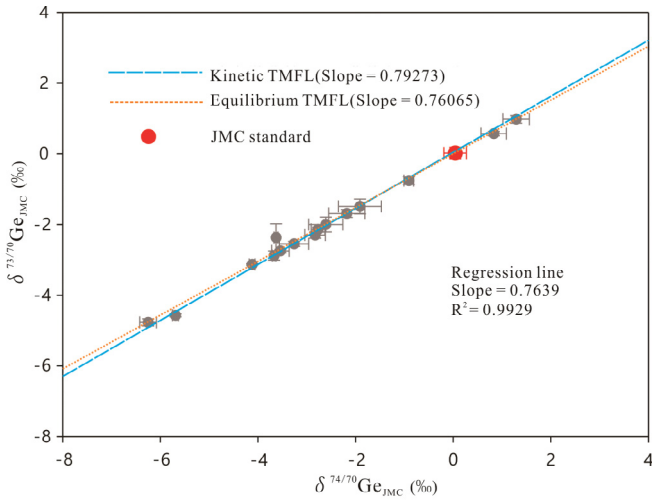

Fig. 4. Relationship between position of measured sample and mass fractionation curve (TMFL) of equilibrium fractionation and kinetic fractionation theory.

5. Discussion

5.1. Occurrence of Ge in sphalerite

Germanium shows chalcophile, lithophile, and organic behavior in nature, and its occurrence is rather complicated (Tu et al., 2003; Bernstein,1985; Höll et al., 2007; Rakov, 2015). In Pb–Zn deposits, some studies suggested that galena is one of the Ge-bearing sulfide basing on the electron microprobe analysis (Fu et al., 2004; Zhou et al, 2008; Wang et al., 2008, 2009, 2010). However, chemical analysis has shown a positive correlation between Ge and Zn in galena, but lack a linear relationship between Ge and Pb in sphalerite, indicating that Ge is mainly hosted in sphalerite, and the Ge in galena is predominately related to the sphalerite micro-inclusions presented within galena (Zhang et al., 2012). Indeed, detailed microscopic and scanning electron microscopic studies on sulfide from the Fule deposit suggested that micro-fine sphalerite grains are surrounded by galena at a microscopic scale, and this can likely be interpreted that some dispersed elements frequently occur in galena (such as Cd) (detailed description in Zhu et al., 2017). The LA-ICP-MS analyses and Ge oxidation state analyses on sphalerite have shown that Ge mainly occupies divalent tetrahedral positions in the sphalerite crystal lattice in the form of tetravalent caption (Ge^{4+}) combined with monovalent metallic cations (such as $3Zn^{2+} \leftrightarrow Ge^{4+} + 2Cu^{+}$) (Belissont et al., 2014, 2016). In the Fule deposit, we observed a negative correlation between the Ge and Cd contents (Fig. 5A). Ge and Cd mainly enter sphalerite by substituting for Zn in the form of isomorphism, and when the Cd content is relatively high, the number of tetravalent Ge cations that substitute the divalent ionic lattice of Zn are relatively restricted and reduced, which leads to a reduction in the Ge content. This indicates that during the formation of sphalerite, Cd and Ge may have competitively replaced the lattice position of Zn in sphalerite. Cd can directly substitute for Zn with respect to its lattice position (Cook et al., 2009; Ye et al., 2011) but Ge needs to cooperate with other elements (such as Cu) to replace Zn lattice position (Belissont et al., 2016). Therefore, it is relatively easy for Cd to enter into the sphalerite crystal lattice, which causes Ge that enters sphalerite to be "suppressed". As the entry of metallic elements into the lattice of sphalerite is an elusive process that is restricted by the various physical and chemical properties of ore-forming fluids (Wen et al., 2016), and the controlling mechanisms on the Ge content changes in sphalerite need further study.

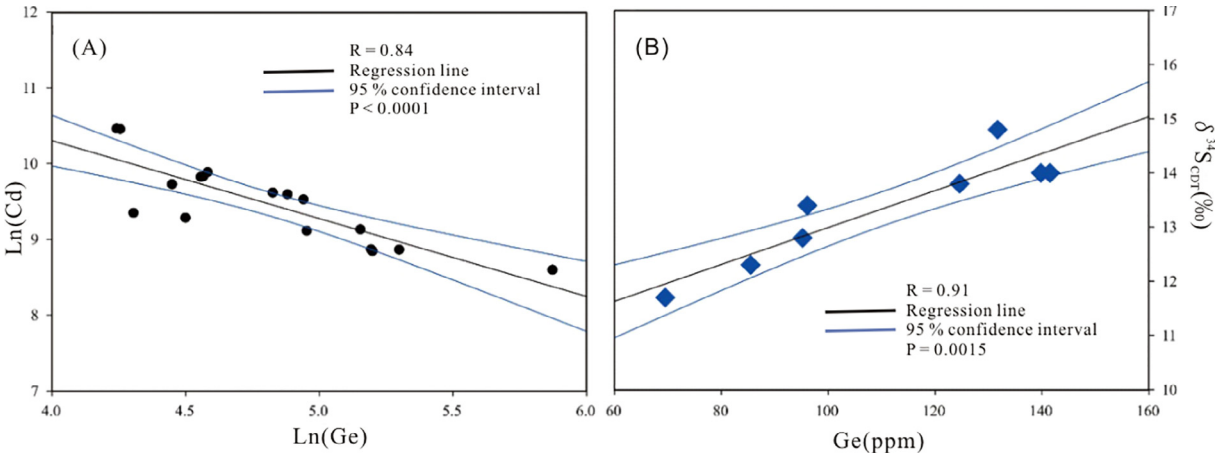

Fig. 5. Relationship between (A) Ge and Cd contents and (B) Ge contents and sulfur isotope compositions in sphalerite from the Fule deposit (some samples in Fig. 5A are cited from Zhang et al., 2012).

In Pb–Zn deposits, Ge can also exist in the form of independent Ge-minerals. For example, Zhang et al. (2008) discovered individual minerals of Ge (GeO2, 39.84%; Al2O3, 49.96%) associated with sphalerite and pyrite in the Huize Pb–Zn deposit. Although single minerals of Ge have not been reported in the Fule deposit, we conclude that the form of independent Ge-minerals can also be ignored relative to isomorphous Ge-minerals. First, no Ge independent minerals were reported in previous studies (Si, 2005; Zhu et al., 2017). Second, sphalerite is the predominant sulfide that contains Ge and Cd in the Fule deposit, and if Ge occurs as independent Ge minerals, the good negative correlation between Ge and Cd is not likely be observed.

Previous studies have shown that there are regular variations in the Cd concentrations of different colored sphalerites within the same hand specimen, and dark sphalerite has a higher Cd concentration than lighter one (Belissont et al., 2014; Zhu et al., 2017). However, the samples collected from the Fule deposit have no regular variation in the Ge concentrations between different colored sphalerites. Belissont et al. (2014) studied different colored sphalerite in the Noailhac-Saint-Salvy deposit in France and found that dark sphalerite has relatively higher Ge contents than light sphalerite, and that the Ge content of dark-brown banded sphalerite varies from 59 ppm to 2576 ppm. In contrast, changes in the Ge content of light-brown banded sphalerite vary from 0 ppm (below the detection limit of the instrument) to 1801 ppm (Belissont et al., 2014). This result suggests the heterogeneous distribution of Ge contents at a microscope scale, which may be responsible for the irregular changes in Ge concentrations between different colored sphalerites in the Fule deposit.

Interestedly, we found a positive correlation between the Ge content and $\delta^{34}S_{CDT}$ value (Fig. 5B), with an R value of 0.91 and a P value of 0.0015, which indicates a significant correlation. This relationship has not been reported previously in Pb-Zn deposits. Due to limited studies on Ge in hydrothermal systems, we cannot give a powerful explanation on this correlation, but we suggest that fluid temperature is most likely a key factor that results in such a positive correlation: (1) S isotope system has been well established in hydrothermal systems in the past decades and fluid temperature is one of the key factor that controls S isotope fractionation factor ($\alpha_{sphalerite\text{-}solution}$) (Ohmoto, 1972; Clayton, 1981); (2) recent reviews on trace elements in sphalerite from different types of deposits show that trace elements in sphalerite are strongly controlled by fluid temperature rather than salinity or source-rock composition, particularly with respect to the concentrations of Ge (Frenzel et al., 2016). Thus, we conclude that the positive correlation most likely results from the variation of fluid temperature in the Fule deposit.

5.2. Relationships between Ge and Cd isotopes

Compared with previously reported Ge isotopic data in Pb-Zn deposits, we determined that the sphalerite in the Fule deposit is enriched in lighter $\delta^{74/70}$Ge values (−6.57‰ to 0.97‰) than other Pb–Zn deposits in the SYG area, where the $\delta^{74/70}$Ge values in the Shanshulin Pb–Zn deposit vary from − 1.71 to 2.07‰, and the $\delta^{74/70}$Ge values in Tianqiao range from − 3.18 to 0.54‰ (Meng et al., 2015). Li et al. (2009) calculated the fractionation factors of Ge from a combination of different ionic clusters and suggested that it is easy to enrich the Ge-S perssad with light Ge isotope, and this is an important reason why light isotopes are enriched in sulfides.

Meng et al. (2015) found fractionation of the Ge isotope among different minerals and the preferential trend of enrichment of light Ge isotopes in sulfides is $\delta^{74/70}Ge_{pyrite} < \delta^{74/70}Ge_{sphalerite} < \delta^{74/70}Ge_{galena}$. They inferred that this phenomenon is related to the relative abundance of various minerals and the mineralization sequence. However, as previously mentioned, the average contents of Ge in sphalerite are several tens of times (or even several hundred times) higher than that of other sulfides such as galena (Zhang et al., 2012; seen in Table 3). Therefore, we consider that this phenomenon can be explained by investigating the occurrence of other dispersed elements in Pb–Zn deposits, such as Cd. Zhu et al. (2017) investigated the compositions of the Cd isotope in galena and found that although the Cd content of galena differs, there is a significant positive correlation between Cd and the Zn contents. This is because that Cd is mainly hosted in sphalerite, and micro inclusions of sphalerite are commonly enclosed in galena, resulting in the positive correlation between Cd and the Zn contents in galena. It is thus proposed that differences in Cd isotope fractionation between galena and sphalerite in the same hand specimen are related to differences in Cd isotope compositions in the different stages of sphalerite (Zhu et al., 2017). In addition, Zhang et al. (2012) determined the contents of Ge in galena from six typical Pb–Zn deposits in Sichuan–Yunnan–Guizhou province. Chemical analysis showed an excellent linear correlation between Ge and Zn, and they concluded that the Ge in galena originates from micro inclusions of sphalerite surrounded by galena. Consequently, the reason why Ge isotope fractionation exists between different minerals (except sphalerite) can be explained by the differences in the Ge isotope composition of sphalerite inclusions within sulfides. Belissont et al. (2014) found a good positive correlation between the Ge content and Ge isotope composition of sphalerite, and considered that the changes in the Ge isotope composition occurred in relation to Rayleigh fractionation. Through studying the different sphalerites in the Fule Pb–Zn deposit, it is evident that light Ge isotopes are more likely to be enriched in dark sphalerite (Fig. 6A), and this behavior is similar to that of Cd isotopes (Fig. 6B).

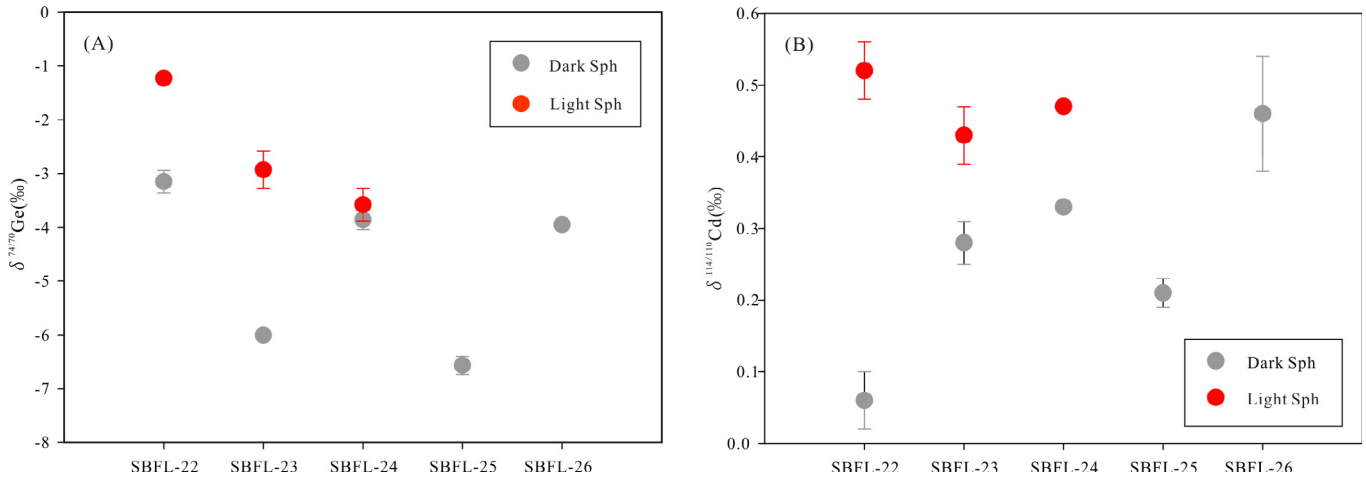

Fig. 6. (A) Ge isotope compositions and (B) Cd isotope compositions in sphalerite from early and late-stage sphalerite.

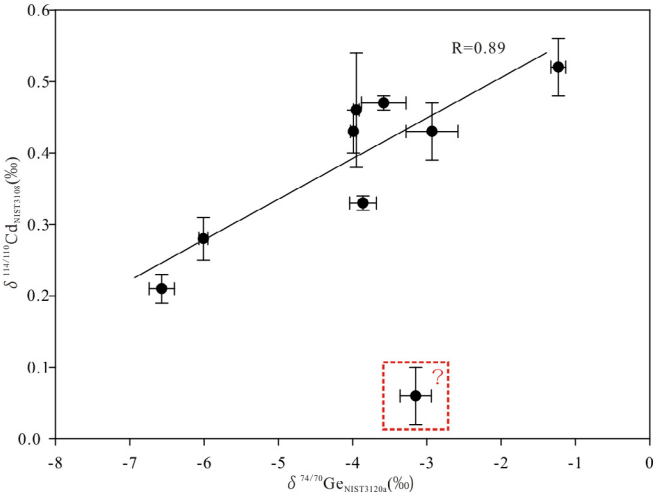

Fig. 7. Correlation between Cd and Ge isotopic compositions of sphalerite from Fule deposit.

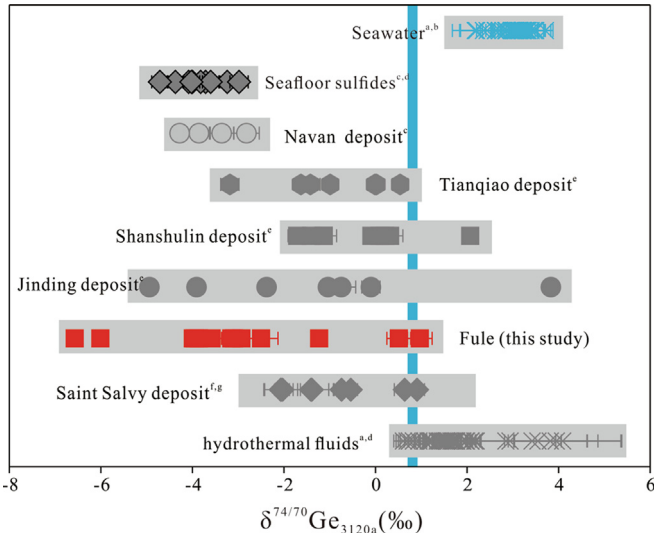

Fig. 8. Comparison of Ge isotopic composition of sulfides from different deposits, as well as other end-members that related to hydrothermal systems. The blue vertical bar represents the Ge isotopic composition of BSE (Ge = 0.59 ± 0.18‰) (Escoube et al., 2012). Data sources: [a]Baronas et al. (2017); [b]Guillermic et al. (2017); [c]Escoube et al. (2012); [d]Escoube et al. (2015); [e]Meng et al. (2015); [f]Belissont et al. (2014); [g]Luais et al. (2012). (For interpretation of the references to color in this figure legend, the reader is referred to the web version of this article.)

This phenomenon demonstrates that early stage sphalerite is relatively enriched in light Ge isotopes whereas late sphalerite is relatively enriched in heavy Ge isotopes, which implies that Ge isotope fractionation may be controlled by Rayleigh fractionation. A comparison between Ge and Cd isotopes shows that all samples (except for SBFL-22 dark sphalerite) fall near the regression line with R = 0.89 (Fig. 7), thus indicating a significant correlation between the two metal isotopes. Therefore, all were controlled by Rayleigh distillation.

5.3. Potential Ge sources in the deposit

In mid ocean ridge hydrothermal systems, metal sources of seafloor sulfide are relatively simple in comparison with arc and ancient hydrothermal systems (e.g., MVT deposits). Previous studies have shown that basement rocks and seawater are the dominant metal sources for seafloor sulfide (Hannington et al., 2005 and reference there in). Baronas et al. (2017) reported Ge isotope compositions of hydrothermal fluids from high-T and low-T systems, and found that the average $\delta^{74/70}$Ge values from the two systems are 1.5 ± 0.4 and 3.5 ± 0.5‰, respectively, which are much higher than the Bulk Silicate Earth (BSE) (0.59 ± 0.18‰; Escoube et al., 2012; Fig. 8). However, seafloor sulfides from mid ocean ridge hydrothermal systems are rich in light Ge isotopes with $\delta^{74/70}$Ge values ranging from −3.60 to −4.71‰ (Escoube et al., 2015; Fig. 8). These results indicate that sulfide precipitation could result in large Ge isotope fractionation with $\Delta^{74/70}$Ge up to 5.6 ± 0.6‰ (2SD) (Escoube et al., 2015) because Ge-S perssad could strongly rich in light Ge isotope (Li et al., 2009). In the SYG area, two end-members, the sediments and the Emeishan basalts, are suggested as the metal sources of the Pb-Zn deposits (Xu et al., 2014 and reference therein); however, trace metal sources in the Pb-Zn deposits are still in controversial. Although we did not measure the Ge isotope composition of the sediments, Ge isotope composition of seawater could be used to represent that of carbonate due to minor fractionation between seawater and sediment with an average $\delta^{74/70}Ge_{seawater}$ value of 3.03 ± 0.28‰ (Guillermic et al., 2017; Baronas et al., 2017). Due to homogenous Ge isotope compositions in igneous rocks (Escoube et al., 2012), we estimate that the Emeishan basalts have similar Ge isotope compositions to the BSE with an average $\delta^{74/70}Ge_{basalt}$ values of 0.59 ± 0.18‰. In the Fule deposit, the average $\delta^{74/70}Ge_{sphalerite}$ value is −3.3 ± 0.22‰ (2SD) and we reasonably assume that $\Delta^{74/70}Ge_{spahlerite\text{-}fluid}$ is −5.6‰ during sulfide precipitation. Thus, the $\delta^{74/70}Ge_{fluid}$ of ore-forming fluid is estimated to ~2.3‰. We assume that there are negligible Ge isotope fractionations between ore-forming fluid

and source rock, thus, most Ge in sphalerite was likely derived from mixing fluids, and sediment is likely the dominant Ge source in the Fule deposit. This conclusion is consistent with newly published studies on the Fule deposit (Zhu et al., 2017; Zhou et al., 2018).

Fig. 8 here

6. Conclusions

(1) The Ge concentrations of sphalerite from the Fule deposit range from 60 ppm to 141.5 ppm. In contrast, there are large variations in the $\delta^{74/70}$Ge values in sphalerite from the Fule deposit, ranging from −6.57‰ to 0.97‰. In addition, one value we reported in this study has the lowest $\delta^{74/70}$Ge value in comparison with the published data in sulfides.
(2) There is a negative correlation between Ge and Cd concentrations in sphalerite, which may be resulted from that Cd is easier than Ge to incorporate into sphalerite and Ge is difficult to substitute for Zn due to high Cd concentration. We simultaneously observed that the Ge content is closely related to the S isotope, which is mainly controlled by fluid temperature.
(3) A comparison of different sphalerite colors in the same sample specimen shows that dark sphalerite is more enriched in light Ge isotopes than light sphalerite, which is similar to the behavior of the Cd isotope and has a good linearity between Ge and Cd isotopes. It is thus suggested that Cd and Ge isotopic fractionation may similarly be controlled by the Rayleigh process, or they underwent similar geochemical processes. This provides a new insight into the enrichment mechanism of dispersed elements in SYG area.
(4) Based upon previous studies, we give a constraint on the Ge sources in the studied deposit and conclude that Ge is derived from mixing sources and sediment may be the dominant Ge source in the Fule deposit.

Declaration of Competing Interest

The authors declare that they have no known competing financial interests or personal relationships that could have appeared to influence the work reported in this paper.

Acknowledgments

This project was financially supported by the National Key R&D Program of China (No. 2017YFC0602500) and the National Natural Science Foundation of China (No. 41773012). We are very grateful to reviewers from the journal for their helpful comments, which have greatly improved the quality of the manuscript.

Appendix A. Supplementary data

Supplementary data to this article can be found online at https://doi.org/10.1016/j.oregeorev.2020.103466.

References

Baronas, J.J., Hammond, D.E., McManus, J., Wheat, C.G., Siebert, C., 2017. A global Ge isotope budget. Geochemica et Cosmochimica Acta. 203, 265–283.
Baronas, J.J., Torres, M.A., West, A.J., Rouxel, O., Georg, B., Bouchez, J., Gaillardet, J., Hammond, D.E., 2018. Ge and Si isotope signatures in rivers: a quantitative multiproxy approach. Earth Planet. Sci. Lett. 503, 194–221.
Belissont, R., Boiron, M.C., Luais, B., Cathelineau, M., 2014. LA-ICP-MS analyses of minor and trace elements and bulk Ge isotopes in zoned Ge-rich sphalerites from the Noailhac-Saint-Salvy deposit (France): insights on incorporation mechanisms and ore deposition processes. Geochemica et Cosmochimica Acta. 126, 518–540.
Belissont, R., Muñoz, M., Boiron, M.C., Luais, B., Mathon, O., 2016. Distribution and oxidation state of Ge, Cu and Fe in sphalerite by μ-XRF and K-edge μ-XANES: insights into Ge incorporation, partitioning and isotopic fractionation. Geochemica et Cosmochimica Acta 177, 298–314.
Bernstein, L.R., 1985. Germanium geochemistry and mineralogy. Geochemica et Cosmochimica Acta 49 (11), 2409–2422.
Clayton, R.N., 1981. Isotopic thermometry. In: Newton, R.C. (Ed.), Thermodynamics of Minerals and Melts. Speinger Verlag, New York, pp. 85–109.
Cook, N.J., Ciobanu, C.L., Pring, A., Skinner, W., Shimizu, M., Danyushevsky, L., Saini-Eidukat, B., 2009. Trace and minor elements in sphalerite: a LA-ICPMS study. Geochemica et Cosmochimica Acta 73 (16), 4761–4791.
Cui, Y.L., Zhou, J.X., Huang, Z.L., Luo, K., Nian, H.L., Ye, L., Li, Z.L., 2018. Geology, geochemistry and ore genesis of the Fule Pb-Zn deposit, Yunnan Province, Southwest China. Acta Petrologica Sinica 34 (1), 194–206.
Escoube, R., Rouxel, O.J., Luais, B., Ponzevera, E., Donard, O.F.X., 2012. An intercomparison study of the germanium isotope composition of geological reference materials. Geostand. Geoanal. Res. 36 (2), 149–159.
Escoube, R., Rouxel, O., Edwards, K., Glazer, B., Donard, O., 2015. Coupled Ge/Si and Ge isotope ratios as geochemical tracers of seafloor hydrothermal systems: case studies at Loihi Seamount and East Pacific Rise 9°5′N. Geochemica et Cosmochimica Acta 167, 93–112.
Frenzel, M., Hirsch, T., Gutzmer, J., 2016. Gallium, germanium, indium, and other trace and minor elements in sphalerite as a function of deposit type–a meta-analysis. Ore Geol. Rev. 76, 52–78.
Fu, S.H., Gu, X.X., Wang, Q., Li, F.Y., Zhang, M., 2004. A preliminary study on the enrichment regularity of dispersed elements in lead-zinc deposits in the SW margin of the yangtze platform. Bull. Mineral., Petrol. Geochem. 23 (2), 105–108 (in Chinese with English abstract).
Galy, A., Pomiès, C., Day, J.A., Pokrovsky, O.S., Schott, J., 2003. High precision measurement of germanium isotope ratio variations by multiple collector–inductively coupled plasma–mass spectrometry. J. Anal. At. Spectrom. 18, 115–119.
Green, M.D., Rosman, K.J.R., DeLaeter, J.R., 1986. The isotopic composition of germanium in terrestrial samples. Int. J. Mass Spectrom. Ion Processes 68, 15–24.
Guillermic, M., Lalonde, S.V., Hendry, K.R., Rouxel, O.J., 2017. The isotope composition of inorganic Germanium in seawater and deep sea sponges. Geochemica et Cosmochimica Acta. https://doi.org/10.1016/j.gca.2017.06.011.
Han, R.S., Liu, C.Q., Huang, Z.L., Chen, J., Ma, D.Y., Lei, L., Ma, G.S., 2007. Geological features and origin of the Huize carbonate-hosted Zn–Pb–(Ag) district, Yunnan, South China. Ore Geol. Rev. 31, 360–383.
Hannington, M.D., de Ronde, C.E.J., Petersen, S., 2005. Sea-floor tectonics and submarine hydrothermal systems: ECONOMIC GEOLOGY 100TH ANNIVERSARY VOLUME, p. 111 − 141.
Höll, R., Kling, M., Schroll, E., 2007. Metallogenesis of germanium—a review. Ore Geol. Rev. 30 (3–4), 145–180.
Hu, R.Z., Fu, S.L., Huang, Y., Zhou, M.F., Fu, S.H., Zhao, C.H., Wang, Y.J., Bi, X.W., Xiao, J.F., 2017. The giant South China Mesozoic low temperature metallogenic domain: Reviews and a new geodynamic model. J. Asian Earth Sci. 137, 9–34.
Huang, Z.L., Li, W.B., Chen, J., Xu, D.R., Han, R.S., Liu, C.Q., 2004. Carbon and Oxygen isotope geochemistry of the Huize superlarge Pb-Zn ore deposits in Yunnan province. Geotectonica et Metallogenia 28 (1), 53–59 (in Chinese with English abstract).
Jing, Z.G., 2008. Ore controlling factors, metallogenic regularity and Prospecting Prediction of Pb-Zn deposits in Northwest Guizhou. Metallurgical Industry Press, Beijing 1–109 (in Chinese).
Li, X., Zhao, H., Tang, M., Liu, L., 2009. Theoretical prediction for several important equilibrium Ge isotope fractionation factors and geological implications. Earth Planet. Sci. Lett. 287 (1), 1–11.
Li, Z.L., Ye, L., Huang, Z.L., Zhou, J.X., Hu, Y.S., Nian, H.L., 2018. Mineralogical characteristics and geological significance of copper minerals in fule Pb-Zn deposit, Yunnan province, China. Geol. J. China Univ. 24 (2), 200–209 (in Chinese with English abstract).
Liang, F., Bi, X.W., Feng, C.X., Tang, Y.Y., Wei, D.X., Dai, Z.H., 2016. Mineralogical and geochemical characteristics of carbonate and implications for ore-forming mechanism of the Fule Pb-Zn deposit, Yunnan Province, China. Actor Petrologica Sinica 32 (11), 3418–3430 (in Chinese with English abstract).
Liu, J.D., Zhang, C.J., Liu, X.F., Li, Y.G., Yang, Z.X., Wu, D.C., 2004. Metallogenic regularity and prospecting direction of Southwest margin of Yangtze platform. Geology Press, Beijing, pp. 1–204 (in Chinese).
Liu, Y.Y., Qi, L., Gao, J.F., Ye, L., Huang, Z.L., Zhou, J.X., 2015. Re-Os dating of galena and sphalerite from lead-zinc sulfide deposits in Yunnan Province, SW China. J. Earth Sci. 2 (3), 343–351.
Lü, Y.H., Han, R.S., Ren, T., Qiu, W.L., Rang, H., Gao, Y., 2015. Ore-controlling characteristics of fault Structures and their relation to mineralization at Fulechang Zn-Pb mining district in deposit concentration district of Northeastern Yunnan China. Geoscience 29 (3), 563–575 (in Chinese with English abstract).
Luais, B., 2012. Germanium chemistry and MC-ICPMS isotopic measurements of Fe–Ni, Zn alloys and silicate matrices: insights into deep Earth processes. Chem. Geol. 334, 295–311.
Meng, Y.M., Hu, R.Z., 2017. Minireview: advances in germanium isotope analysis by multiple collector-inductively coupled PlasmA-mass spectrometry. Anal. Lett. https://doi.org/10.1080/00032719.2017.1350965.
Meng, Y.M., Qi, H.W., Hu, R.Z., 2015. Determination of germanium isotopic compositions of sulfides by hydride generation MC-ICP-MS and its application to the Pb–Zn deposits in SW China. Ore Geol. Rev. 65, 1095–1109.
Nian, H.L., Cui, Y.L., Li, Z.L., Jia, F.J., Chen, W., Yang, S.X., Yang, Z., 2017. Area and outskirts in Luoping area, Eastern Yunnan Province China. Acta Mineralogica Sinica 37 (4), 469–474 (in Chinese with English abstract).
Ohmoto, H., 1972. Systematics of sulfur and carbon isotopes in hydrothermal ore deposits. Econ. Geol. 67, 551–579.
Qi, H.W., Hu, R.Z., Jiang, K., Zhou, T., Liu, Y.F., Xiong, Y.W., 2019. Germanium isotopes and Ge/Si fractionation under extreme tropical weathering of basalts from the Hainan Island, South China. Geochimi. Cosmochim. Acta. https://doi.org/10.1016/j.gca.2019.03.022.

Qi, H.W., Rouxel, O., Hu, R.Z., Bi, X.W., Wen, H.J., 2011. Germanium isotopic systematics in Ge-rich coal from the Lincang Ge deposit, Yunnan Southwestern China. Chem. Geol. 286, 252–265.
Rakov, L.T., 2015. Role of germanium in isomorphic substitutions in quartz. Geochem. Int. 53 (2), 171–181.
Reynolds, J.H., 1953. The isotopic constitution of silicon, germanium, and hafnium. Phys. Rev. 90, 1047–1049.
Rosman, K.J.R., Taylor, P.D.P., 1998. Isotopic compositions of the elements 1997 (Technical Report). Pure Appl. Chem. 70, 217–235.
Rouxel, O.J., Luais, B., 2017. Germanium isotope geochemistry. Rev. Mineral. Geochem. 82 (1), 601–656.
Rouxel, O., Galy, A., Elderfield, H., 2006. Germanium isotopic variations in igneous rocks and marine sediments. Geochemica et Cosmochimica Acta 70, 3387–3400.
Si, R.J., 2005. Ore deposit geochemistry of the Fule dispersed element-polymetallic deposit, Yunnan Province. Guiyang: Institute of Geochemistry, Chinese Academy Sciences, pp. 1–126 (Ph.d. Thesis) (in Chinese with English abstract).
Si, R.J., Gu, X.X., Pang, C.C., Fu, S.H., Li, F.Y., Zhang, M., Li, Y.H., Li, X.Y., Li, J., 2006. Geochemical character of dispersed element in sphalerite from Fule Pb-Zn polymetal deposit Yunnan Province. J. Mineral Petrol. 26 (1), 75–80 (in Chinese with English abstract).
Siebert, C., Ross, A., McManus, J., 2006. Germanium isotope measurements of high-temperature geothermal fluids using double-spike hydride generation MC-ICP-MS. Geochemica et Cosmochimica Acta 70, 3986–3995.
Taylor, S.R., McClennan, S.M., 1985. The Continental Crust: Its Composition and Evolution. Blackwell Scientific Publications, pp. 67.
Tu, G.Z., Gao, Z.M., Hu, R.Z., Zhang, Q., Li, C.Y., Zhao, Z.H., Zhang, B.G., 2003. Disperse Element Geochemistry and Mineralization Mechanism. Geological Publishing House, Beijing 1–430 (in Chinese).
Wang, Q., An, Y.L., Gu, X.X., Fu, S.X., Li, F.Y., Yang, H.Y., 2010. Enrichment of the dispersed elements Cd, Ge and Ga in the Daliangzi Lead-Zinc deposit, Huidong Sichuan. Sedimentary Geol. Tethyan Geol. 30 (1), 78–84 (in Chinese with English abstract).
Wang, Q., An, Y.L., Gu, X.X., Fu, S.X., Li, F.Y., 2009. Enrichment law of the dispersed elements Gd, Ge and Ga in the Tianbaoshan Pb-Zn deposit, Sichuan, China. J. Chengdu Univ. Technol. (Science & Technology Edition) 36 (4), 395–401 (in Chinese with English abstract).
Wang, Q., Gu, X.X., Fu, S.H., Zhang, M., Li, F.Y., 2008. Enrichment of the dispersed elements Cd, Ge and Ga in the Huize lead-zinc deposit Yunnan. Sedimentary Geology and Tethyan Geology 28 (4), 69–73 (in Chinese with English abstract).
Wen, H.J., Zhu, C.W., Zhang, Y.X., Cloque, C., Fan, H.F., Fu, S.H., 2016. Zn/Cd ratios and cadmium isotope evidence for the classification of lead-zinc deposits. Sci. Rep. https://doi.org/10.1038/srep25273.
Xiong, S.F., Gong, Y.J., Jiang, S.Y., Zhang, X.J., Li, Q., Zeng, G.P., 2018. Ore genesis of the Wusihe carbonate-hosted Zn-Pb deposit in the Dadu River Valley district, Yangtze Block, SW China: evidence from ore geology, S-Pb isotopes, and sphalerite Rb-Sr dating. Miner. Depos. 53, 967. https://doi.org/10.1007/s00126-017-0776-y.
Xu, Y., Huang, Z., Zhu, D., Luo, T., 2014. Origin of hydrothermal deposits related to the Emeishan magmatism. Ore Geol. Rev. 63, 1–8.
Ye, L., Nigel, J.K., Cristiana, L.C., Liu, Y.P., Zhang, Q., Liu, T., Gao, W., Yang, Y.L., Danyushevsky, L., 2011. Trace and minor elements in sphalerite from base metal deposits in South China: A LA-ICPMS study. Ore Geol. Rev. 39, 188–217.
Young, E.D., Galy, A., Nagahara, H., 2002. Kinetic and equilibrium mass-dependent isotopic fractionation laws in nature and their geochemical and cosmochemical significance. Geochemica et Cosmochimica Acta 66 (6), 109–1104.
Zhang, L.S., Huang, Z.L., Li, X.B., 2008. Discovery of the independent mineral of Germanium in the Huize large-scale Pb-Zn deposit, Yunnan Province, China. Acta Mineralogica Sinica 28 (1), 15–16 (in Chinese with English abstract).
Zhang, Y.X., Zhu, C.W., Fu, S.H., Zhou, G.F., Qin, T.R., Fan, H.F., Wen, H.J., 2012. A study on the enrichment in Sichuan, Regularity of ispersed elements Ge in Pb-Zn deposits Yunnan and Guizhou Provinces, China. Acta Mineralogica Sinica 32 (1), 60–64 (in Chinese with English abstract).
Zhou, J.X., Huang, Z.L., Li, X.B., Zhou, G.F., Liu, S.R., Zheng, W.Q., 2008. New evidence for the enrichment of Germanium in galena of the Huidong Daliangzi large-scale Pb-Zn deposit, Sichuan Province, China. Acta Mineralogica Sinica 28 (4), 473–475 (in Chinese with English abstract).
Zhou, J.X., Huang, Z.L., Zhou, M.F., Li, X.B., Jin, Z.G., 2013. Constraints of C-O-S-Pb isotope compositions and Rb-Sr isotopic age on the origin of the Tianqiao carbonate-hosted Pb-Zn deposit, SW China. Ore Geol. Rev. 53, 77–92.
Zhou, J.X., Huang, Z.L., Zhou, M.F., Zhu, X.K., Muchez, P., 2014. Zinc, sulfur and lead isotopic variations in carbonate-hosted Pb-Zn sulfide deposits, Southwest China. Ore Geol. Rev. 58, 41–54.
Zhou, J.X., Luo, K., Wang, X.C., Wilde, S.A., Wu, T., Huang, Z.L., Cui, Y.L., Zhao, J.X., 2018. Ore genesis of the Fule Pb Zn deposit and its relationship with the Emeishan Large Igneous Province: evidence from mineralogy, bulk C-O–S and in situ S–Pb isotopes. Gondwana Res. 54, 161–179.
Zhu, C.W., Wen, H.J., Fan, H.F., Zhang, Y.X., Liu, J., Yao, T., Wang, G.H., 2014. Chemical pretreatment methods for measurement of Ge isotopic ratio on sphalerite in Lead-Zinc deposits. Rock Mineral Anal. 33 (3), 305–311 (in Chinese with English abstract).
Zhu, C.W., 2014b. Geochemistry of Cd and Ge, and Their Isotope in Carbonate-hosted Lead-Zinc Ore Deposits in the Boundary Area of Sichuan, Yunnan and Guizhou Provinces, China. Institute of Geochemistry, Chinese Academy Sciences, Guiyang (Ph.d. thesis) (in Chinese with English abstract).
Zhu, C.W., Wen, H.J., Zhang, Y.X., Hu, S.H., Fan, H.F., Cloquet, C., 2017. Cadmium isotope fractionation in the Fule Mississippi Valley-type deposit, Southwest China. Mineralium Deposita 52 (5), 675–686.
Zhu, C.W., Wen, H.J., Zhang, Y.X., Yin, R.S., Cloquet, C., 2018. Cd isotope fractionation during sulfide mineral weathering in the Fule Zn-Pb-Cd deposit, Yunnan Province, Southwest China. Sci. Total Environ. 616–617, 64–72.